# IMECE2022-95942

## **CELLULAR LATTICES WITH STRUTS AND PLATES**

Nandika Anne D'Souza University of North Texas Denton, TX Mahan Ghosh University of North Texas Denton, TX

#### **ABSTRACT**

Lightweighting through the creation of porous architectures has been employed extensively in materials such as foams and aerogels. The use of two-dimensional columnar systems such as honeycombs and their related polygons have been employed due to the ease of manufacturing using large scale calendaring. More recently the availability of 3d printing led to a resurgence of cellular architectures that are based on struts. Systems have been explored using atomic lattice mimicry and named as face centered cubic, body centered cubic or simple cubic. The utilization of faces has also been explored paired to the struts. In this paper we explore the effect of gradual face insertion into a body centered cubic lattice. We examine a single cell oriented such as that the faces are arranged around the centroid of the cube. A 4x4x4 lattice is then explored to examine stress transfer to the nearest neighbor. The results present a novel approach to mitigating the challenge with stress concentration that has limited the strut-based lattices in Fused Deposition Modeling (FDM) printing as all systems with faces show significant benefits in modulus, stress and energy absorption enhancement over the pure strut-based lattice.

Keywords: Additive manufacturing, lightweighting, cellular lattice

### 1. INTRODUCTION

Lightweighting structures is vital for fuel economy in aerospace, automotive and other transportation applications as well as in conveying products from one point to another. Porosity has been a frequent solution. Cellular materials have been invaluable for a variety of characteristics such as thermal insulation, acoustic absorption, energy absorption and impact performance. [1, 2] Polymer foams comprise high volume markets such as cushions, food trays, cups to the automotive

interiors. Gibson and Ashby [3] describe a cellular solid as one made of an interconnected network of solid struts or plates or walls which form the edges of faces of cells. Three topographies emerge. Prismatic cells such as honeycombs in two dimensions and a thickness in the third, open cellular structures formed from only struts and closed cellular structures when the cell walls form the boundaries. The combination of cellular architecture, be it prismatic, open or closed cell and intrinsic material properties of the material comprising the cells is further affected by aspects such as cell wall or strut thickness and cell size. In the case of open and close celled foams, the stochastic nature of cell size, cell shape, interconnectedness, wall thickness makes attribution of cause and effect of performance challenging. This has led to the use of density ratios. For example, soft polymer foams that are open cells have density ratios around 0.05 while rigid foams have ratios around 0.2. Increased density ratios are accompanied by more faces and wall thickness. When the density of the foam is more than 30% of the bulk material, the material begins to have less porous structures. We have recently explored the use of physical foaming of poly lactic acid with microcellulose using carbon dioxide [4] where the thermal conductivity in the cellular foams was significantly impacted with cell wall thickness while compression modulus was affected by intrinsic properties of the polymer comprising the walls as well as cellular architecture. This highlights the challenges facing design engineers in formulating structural solutions using stochastic foams.

The advent of 3d printing has led to more exploration of architectures of cellular materials. Honeycombs and other columnar systems are transitioning from non-prismatic cellular structures to periodic lattice structures. Periodic lattice structures describe structures formed by repeating unit cells designed in three orthogonal directions. The unit cell is an interconnected network of ligaments or struts [3,5]. The mechanical behavior

of the interconnected network is affected by the architecture of the repeating unit and was ascribed to connectivity and defined by the Maxwell equation. The equation for three dimensions governing is described by equation 1.

$$M = s - 3j + 6 \tag{1}$$

where s is the number of struts and j is the number of nodes or joints.

Two responses were considered. Using a brick like distribution of cells, Ashby concluded that struts would respond either in bending or in axial deformation based on the constraints imposed on the joints. If a joint was unrestrained in any degree of freedom, the lack of resistance would affect the deformation mode of the connected structure and stretching would ensure. Constraints to displacement introduced by the addition of struts would induce bending deformation. Since occupied volume would affect density, Ashby set relationships that scaled modulus and strength ratios of the cellular lattice to the values of the bulk material to the density ratio of the lattice to the density of the bulk material. He outlined that when  $M \le 0$ , loads are not balanced using equilibrium equations of force and moments. This leads to an imbalance and beams and the frame would have both axial response as well as bending. When M >0, the lattice deforms through an axial stretching response. In further exploration of this concept Ashby established that a lattice that deformed in stretching response would result in three times the stiffness of the lattice that responded in bending. Stretch efficiency would make stretch governed structures more effective for increased modulus to density and strength to weight considerations. Deshpande concluded that cells that are comprised of plates will not impact the stretch and bending response since the plate would contribute as a membrane response and would not contribute to resistance to buckling. Numerous unit cells have been explored by researchers. The simple cubic (SC) architecture of "boxes" has been utilized both as all struts, all plates and hollow struts filled with materials of varying moduli. [6] The body centered cubic (BCC), and the face centered cubic (FCC) have also been extensively investigated. [7-10]. The FCC lattice, particularly due to the 12 struts emanating from a single node, has been further investigated as octet and tetrahedral lattices. When the FCC and BCC lattice is paired to the simple cubic frame, there is a significant increase in mechanical modulus and stress arising from the addition of

The performance of the lattice structures has been significantly impacted by manufacturing defects. For instance, in the all-strut lattices, stress concentration at the nodes has affected properties of the lattice structures while in all plate lattices, closed cells formed with all plates trap hot air leading to poor dimensional accuracy and shape change as the part cools or solidifies. The question that arises is "Can the creation of mixed walls and struts result in lightweight cellular lattice?" To explore this question, we select a BCC-SC or BCCZ unit cell and sequentially add

struts at the same joint. These are termed wither SC-FCC or

FCCZ, SC-BCC or BCCZ. All plate lattices have also been

explored [11] and the results indicate higher modulus and

strength is achieved.

plates to the unit cell. The plates are placed around the cube center and deposition direction is retained for all structures.

#### 2. MATERIALS AND METHODS

Table 1 shows the unit cell of the lattice used in this paper. The nomenclature employed A-B-Q where A represents the polymer (PLA=Polylactic acid), B represents the number of plates (P) in the lattice above and below the midpoint of the cube and Q represents the load direction for compression testing. The direction of the nozzle was also the direction of the load direction. The 2 wall sample has two options for plate placement and therefore an O is added to denote placement of the plates opposite one another.

For all lattice types, a single cell of 10X10 X10 mm with strut diameter of 1.5 mm was utilized. Thus, the single cell had a dimension of 11.5 mm for the x, y and z lengths. Computer Aided Design (CAD) models were first created using Autodesk Inventor professional 2019 then exported in STL format then fed into the Ultimaker Cura 2.0 for slicing and creating the G-code. Each strut cross-section was circular. Ender 3 pro printer by Creality was used to manufacture the samples. The print bed was maintained at 60 °C and the deposition temperature was at 210 °C. The nozzle diameter is 0.4 mm, and all the samples were printed at 100% density. The printing speed was 50mm/s and the layer thickness was maintained at 0.4mm

### 2.1 Mechanical Testing of bulk samples

Bulk samples were tested in tension and compression to determine the modulus using ASTM D638-14, type 1 and ASTM D695-15 respectively. The sample geometry utilized 163 mm length and 50mm gage length for tensile testing and 12.7 mm cylinder diameter and 25.4 mm length for compression testing. The tests were done in triplicate. The Shimadzu Universal Testing Machine was used to test the samples, at a strain rate of 1mm/sec. Flexural tests were conducted in accordance with ASTM D790. A 3-point bend loading configuration was utilized on a Shimadzu AGS-X 10kN machine. The loading rate was kept at 2mm/minute. The force was converted to flexural strength using the formula  $S = 3PL/2bd^2$ , where S = stress at the outer most fiber at midspan, P = load at a given point on the load deflection curve, L = span, b = width of the beam, d = depth ofthe beam. The flexural modulus was calculated using the formula  $E = L^3 m / 4bd^2$ , where E is the Modulus of elasticity. The sample dimensions were chosen as L = 3inch (76.2mm, b = 0.5inch (12.7mm) and d = 3/16inch (4.76mm).

# 2.2 Lattice compression testing

Nomenclature			
PLA-0-Y			
PLA-1-Y			
PLA-2-Y			
PLA-2-O-Y			
PLA-3-Y			
PLA-4-Y			

TABLE 1: LATTICE TYPES, NOMENCLATURE USED

Single and 4X4 lattice elements were fabricated and subjected to compressive loading on the 810 MTS 500kN load capacity, at a strain rate of 1mm/sec, up to complete densification. Three specimens of each sample for compression testing were made and tested, the direction of the print was kept same as the

direction of loading for each sample to eliminate variations due to stepping effect of the FDM printing. From the force-displacement data, the stress-strain data is extracted. The stress values were obtained by dividing the force by overall cross section area of the lattice unit. The strain values were calculated by dividing the total displacement by the overall height of the specimen. Thus, stress strain curves were created using the force displacement curves by dividing the force by 11.5X11.5 mm² for the unit cell and 41.5X41.5 mm² for the 4x4x4 lattice and by 11.5 (unit cell) and 41.5 mm (4x4x4) for the strain. The modulus was calculated using the linear part of the stress-strain curve and averaged for each sample. The specific modulus, strain and energy was calculated by dividing the averaged modulus by the relative density of each lattice type.

# 2.3 Finite Element Modeling

For finite element analysis the models were designed in Autodesk Inventor professional and exported in STEP format and then fed into the Ansys workbench 2019. The lattice was placed in between two structural steel plates and velocity of 1mm/sec was applied to the top plate while keeping the bottom plate static, to mimic the experimental setup. SOLID 187 element type with 10nodes and 3 degrees of freedom was used to mesh the structures with an element size of 0.5mm for unit cells and as 1mm for 4x4x4 as this element has stress stiffening, large deflection, and large strain capabilities. The element sizes were determined using convergence test and maintained uniformly for element types. The compression modulus determined by standard testing is fed into the Ansys workbench as material property for the lattice unit. The contact condition between the plate and the lattice unit was kept as frictional and the coefficient of friction was used 0.1. The force reaction from the bottom plate was extracted and plotted against the strain. The FEA conditions were set based on recommendations by Vanutelli [12].

### 3. RESULTS AND DISCUSSION

The bulk properties of the PLA (Polylactic acid) deposited material are provided in Table 1. The values are close to material properties of compression molded PLA samples that we have previously investigated [4] These were used for the FEA.

	E (GPa)	Yield Stress (MPa)
Tensile	1.04±.04	34.83±2.7
Compression	0.9±.07	56.6±2.9
Flexural	2±.04	43.6±.08

**TABLE 2:** MECHANICAL PROPERTIES OF BULK MATERIAL

The stress-strain plot for the unit cell and 4x4x4 lattice are shown in Figure 1 and b. The slope of both unit cell and 4x4x4 was determined. These are tabulated in Table 3 and plotted in Figure 2. The maximum stress was determined from the data. These are tabulated in Table 4 and plotted for comparative purposes in Figure 3.

The values of the zero-plate lattice (shows a modulus of 65.63 MPa which increases by 21, 50, 54 and 95% over the zeroplate lattice as the plate grows to 1, 2, 3, and 4 plates. The corresponding peak stress undergoes a slight decrease of 8% with 1 plate followed by an increase of 39, 56 and 111% when we go from 0 to 4 plates. Images were captured with a digital camera during the compression test. The deformation response of the zero plate or strut only lattice is strongly affected by buckling of the z strut of the lattice (Figure 4). When plates are present (Figure 5), they fold in an accordion manner while providing enhanced resistance to deformation for the angled struts. The 4x4x4 lattice shows an improvement of 53% over the single cell for the strut-based lattice in modulus and slight loss in stress of 8%. Once plates are placed the increase in modulus is 56, 22 and 110 and 81% over that of the single cell for 1, 2, 3 and 4 plate lattices. The deformation clearly undergoes a change in the scaled up 4x4x4 lattice (Figure 6). In the zero-plate lattice, the deformation reflects limited stress transfer with buckling at the base of the load frame being transmitted rapidly through the structure. When plates are present, the deformation of the entire structure shows a shear type deformation from stress transfer being non uniform across the lattice.

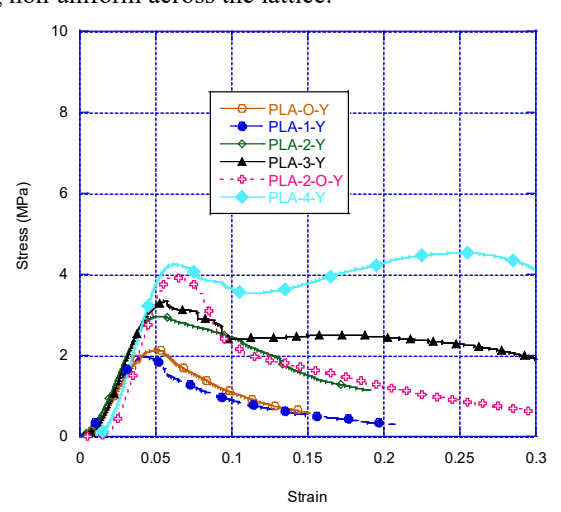


**FIGURE 1a:** STRESS-STRAIN CURVES OF THE UNIT CELL LATTICE

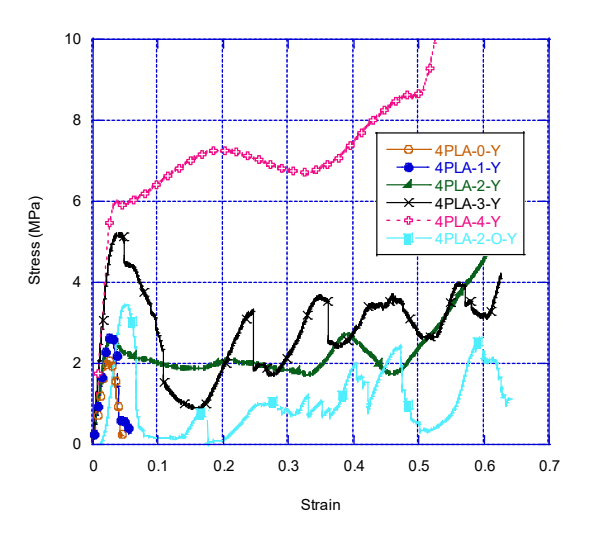


**FIGURE 1b:** STRESS-STRAIN CURVES OF THE 4x4x4 LATTICE

	Experimental		Simulation	
	Single cell	4x4x4	Single cell	4x4x4
	Modulus(MP	Modulus(MPa)	Modulus(	Modulus(
	a)	Modulus(MPa)	MPa)	MPa)
PLA-O-Y	$65.63 \pm 4.12$	$100.13 \pm 1.80$	62.5	41.2
PLA-1-Y	$79.68 \pm 3.98$	$124.41 \pm 0.36$	73.3	47.3
PLA-2-Y	$105.22 \pm 4.02$	$128.29 \pm 3.92$	83	59.7
PLA-2-O-Y	$137.38 \pm 1.52$	$134.25 \pm 4.65$	83.98	54.7
PLA-3-Y	$100.84 \pm 3.73$	$211.60 \pm 5.96$	99.9	77.9
PLA-4-Y	$127.87 \pm 4.37$	$231.85 \pm 24.11$	117.1	100.3

**TABLE 3:** MODULUS OF THE LATTICE

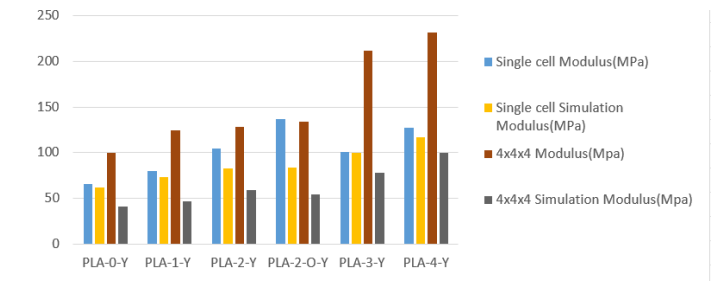


FIGURE 2: AVERAGE MODULI OF LATTICE

	Single cell	4x4x4
	Yield	Yield
	Stress	Stress
	(MPa)	(MPa)
PLA-O-Y	2.14±.39	1.98±0.06
PLA-1-Y	1.96±.41	2.72±0.06
PLA-2-Y	2.97±.39	2.85±0.17
PLA-2-O-Y	4.93±.22	3.41±0.66
PLA-3-Y	3.34±.4	5.43±0.17
PLA-4-Y	4.53±.4	5.41±.52

**TABLE 4:** YIELD STRESS OF THE LATTICE

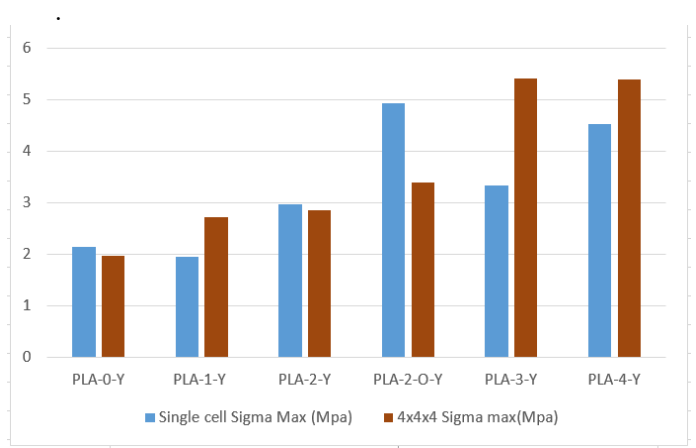


FIGURE 3: AVERAGE YIELD STRESS OF LATTICE

	Single cell	4x4x4
	Sp.	Sp.
	ModulusM	ModulusMpa-
	pa-m^3/kg	m^3/kg
PLA-O-Y	0.29	0.55
PLA-1-Y	0.29	0.50
PLA-2-Y	0.32	0.41
PLA-2-O-Y	0.42	0.43
PLA-3-Y	0.27	0.56
PLA-4-Y	0.30	0.53

**TABLE 5:** SPECIFIC STRESS AND MODULI OF THE LATTICE

The modulus values extracted from simulations indicates around significant deviation in magnitude while similar trend over the experimental values. We note that multiple aspects contribute to the variance. First the values for the bulk PLA is extracted from the tensile and compression samples prepared in the 3D printer. The resulting anisotropy in the sample is not accounted for. The second aspect we note is that manufactured samples fail due to heterogeneities induced by solidification variance as well as geometric variance.

We examine the simulations of the unit cell (Figure 7) and the 4x4x4 lattice and note that the presence of the plates effectively removes the stress concentration around the nodes for all. The weakest link continues to be the buckling for all lattice, but the effect of the plates is to limit the folding or buckling of the struts. Comparing the values of the unit cell and the 4x4x4 cell one can see that scale up is enabled with or without the presence of plates. However, one can note that the 3-plate sample shows the maximum increase in the average yield stress as well as increase in modulus in the scaled sup sample. This indicates that strategically placing plates into lattice while limiting hot spots by completely enclosed all plate lattice in a tetrahedral pocket can also support enhanced stress transfer.

On plotting the energy absorption for the lattice structures tested we found a gradual increase with sequential addition of plates. (Figure 9) The same trends arise in the 4x4x4 structures (Figure 10). Though PLA-2-O-Y and PLA-2-Y have the same density ratio the stark difference in the energy absorption can solely attributed to symmetricity. When two plates are placed symmetrically around the cube center, concurrent benefits in lightweighting and energy absorption are obtained.



**FIGURE 4:** ZERO PLATE LATTICE DEFORMATION SHOWING DOMINANCE OF BUCKLING

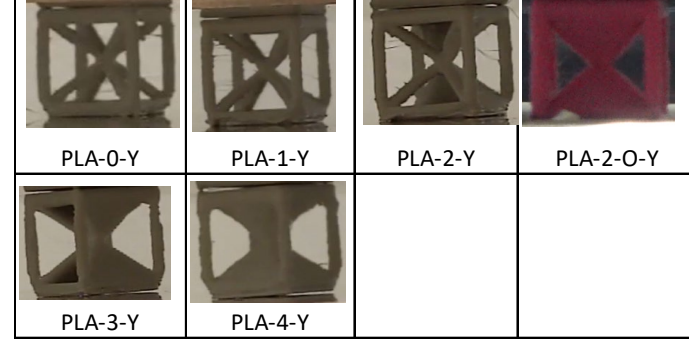
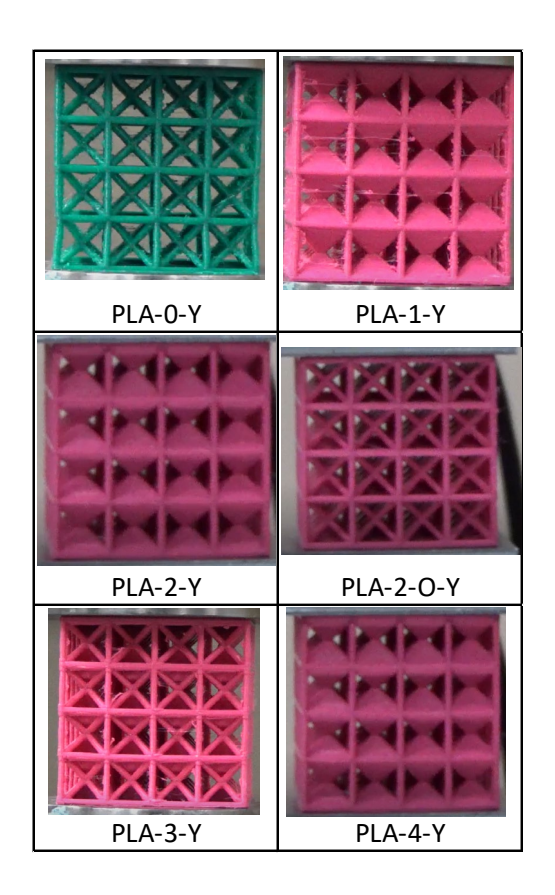
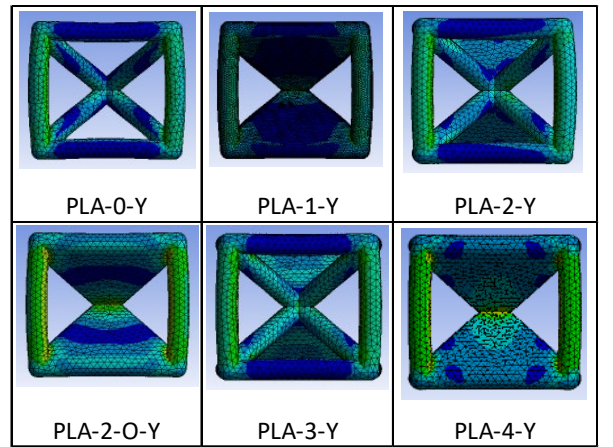


FIGURE 5: UNIT CELL LATTICE UNDER COMPRESSION



**FIGURE 6:** 4X4X4 UNIT CELL UNDER COMPRESSION



**FIGURE 7:** DEFORMATION OF THE UNIT CELL IN THE SIMULATION

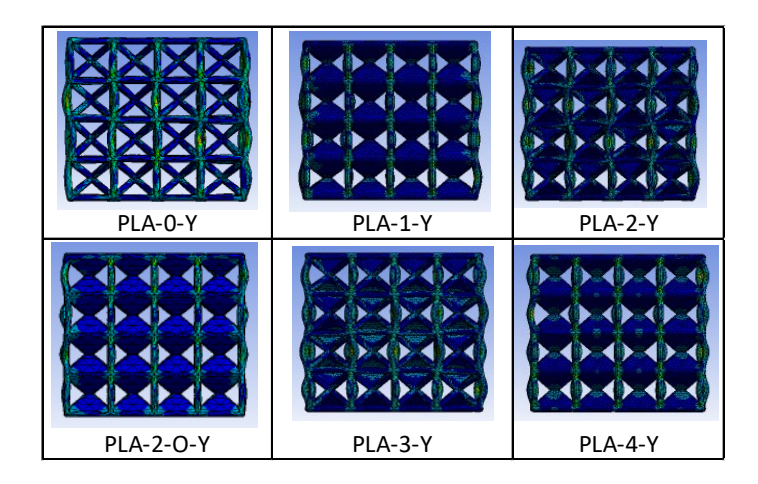


**FIGURE 8:** FEA of the 4x4x4 LATTICE SHOWING STRESS DISSIPATION THROUGH INTRODUCTION OF PLATES.

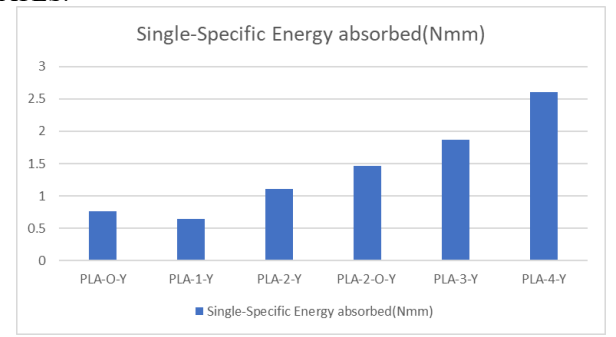


**FIGURE 9:** SPECIFIC ENERGY ABSORPTION IN THE UNIT CELLS

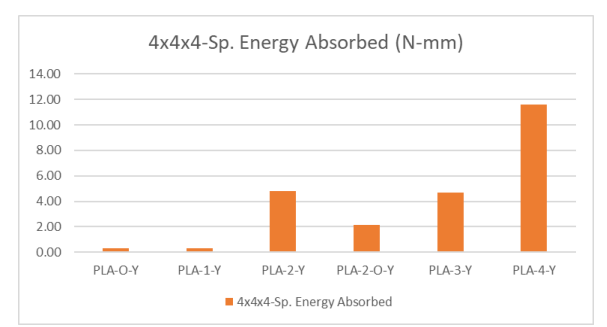


**FIGURE 10:** SPECIFIC ENERGY ABSORPTION IN THE 4X4X4 LATTICE

# 4. CONCLUSION

A strut only and plate only tetrahedral body centered cubic lattice was assessed together with the effect of addition of plates into the strut only lattice. The intermediate strut-plate lattice enables dissipation of heat impeding solidification during deposition. To examine stress transfer and scale up, a 4x4x4 unit cell lattice was also examined. The results indicate that from a perspective of modulus, the modulus of all plate lattice more than

doubles for both the unit cell and a 4x4x4 lattice. The peak stress shows a similar trend of improvement in all plates over all strut lattice in the unit cell and reaches close to 300% improvement in the scaled up 4x4x4 lattice. This indicates that plates serve an important purpose in mitigating the stress concentration and buckling effects in open strut only lattice structures. The systems with plates show similar trends. FDM lattice has a significant effect of solidification which impacts the performance in the scaled up lattice. By comparing a 2 plate that had the plates adjacent versus a 2 plate where the plates were placed opposite each other, there is clear benefit of having symmetry in positioning plates. The new mixed plate and strut architecture

**REFERENCES** 

- [1] T. Maconachie , M. Leary , B. Lozanovski , X. Zhang , M. Qian , O. Faruque , M. Brandt Mater. Des. 183, 2019
- [2] M. Leary, M. Mazur, J. Elambasseril, M. McMillan, T. Chirent, Y. Sun, M. Qian, M. Easton, M. Brandt, Mater. Des., 98, 344, 2016.
- [3] L.J. Gibson, M.F. Ashby, Cellular Solids: Structure and Properties, Cambridge university press, 1997.
- [4] K. Oluwabunmi, N. A. D'Souza, W. Zhao, T. Y. Choi, T. Theyson, Compostable, fully biobased foams using PLA and micro cellulose for zero energy buildings. Sci Rep 10, 17771, 2020.
- [5] M. Ashby, Philos Trans Royal Soc London A: Math Phys Eng Sci 2006;364:15–30.

also showed significant impact on specific energy absorption with a significant increase in energy absorption from addition of plates.

#### 5. ACKNOWLEDGEMENTS

This study was conducted and financially supported by the National Science Foundation. A collaborative research: Engineering Fully Bio-based Foams for the Building Industry. Award number 1728096.

References:

- [6] T. Tacogne-Dejean, D. Mohr, Extreme Mechanics Letters 22, 13, 2018
- [7] S. Xu, J. Shen, S. Zhou, X. Huang, Y.M. Xie, Design of lattice structures with controlled anisotropy, Mater. Des. 93, 443, 2019 [8] M.C. Messner, Optimal lattice-structured materials, J. Mech. Phys. Solids 96, 162, 2016
- [9] T. Tancogne-Dejean, D. Mohr, Elastically-isotropic truss lattice materials of reduced plastic anisotropy, Int. J. Solids Struct., 138 24-39, 2018
- [10] G. Gurtner, M. Durand, Proc. R. Soc. Lond. Ser. A Math. Phys. Eng. Sci. 470, 20130611, 2014.
- [11] J.B. Berger, H.N.G. Wadley, R.M. McMeeking, Mechanical metamaterials at the theoretical limit of isotropic elastic stiffness, Nature 543, 533, 2017.
- [12] R. Vannutelli, Mechanical Behavior of 3D Printed Lattice-Structured Materials, MS Thesis, Youngstown State University (2017)